Synchronized six-step voltage generation in high-speed PMSM drive

Leszek Jarzebowicz
Faculty of Electrical and Control Engineering
Gdansk University of Technology
Gdansk, Poland
leszek.jarzebowicz@pg.edu.pl

Maciej Cisek
Faculty of Electrical and Control Engineering
Gdansk University of Technology
Gdansk, Poland
maciej.cisek@pg.edu.pl

Abstract—**Synchronized voltage generation has already been considered in the context of pulse width modulation (PWM). References prove that synchronized PWM substantially decreases subharmonics in inverter output voltage when operating with low switching-to-fundamental frequency ratio. This paper identifies problems of unsynchronized voltage generation in electric drives under six-step inverter operation. Guidelines for the synchronization scheme were formulated, considering both minimization of voltage subharmonics and drive control properties. A comprehensive algorithm for adjusting the voltage update rate in six-step permanent magnet synchronous motor (PMSM) drive was presented. Superior properties of the synchronized six-step voltage generation were demonstrated by simulation and experiment for an exemplary 5-kW PMSM drive.**

Keywords—electric drives, high-speed drives, permanent magnet synchronous drives, digital signal processing

I. INTRODUCTION

Numerous applications require from the electric drive to operate in an extended speed range associated with flux-weakening control [1][2]. For instance, electric and hybrid cars use flux-weakening to reconcile requirements of high starting torque and high-speed driving capability, without using variable-ratio transmission. Such cars are typically fitted with permanent magnet synchronous motor (PMSM) drives, in which the flux-weakening region covers from 50 to 80% of the whole operational speed range [3].

During flux-weakening control, the drive operates at voltage constraint, so the level of inverter output voltage has a major impact on available motor torque. Six-step control is a solution to increasing the torque by improved utilization of the inverter DC-bus voltage [4]. Six-step control switches the inverter state only six times per output voltage period, so that this voltage is composed from six steady-voltage intervals (Fig. 1b). As the fundamental-frequency component of the six-step voltage is substantially higher than in case of voltage modulation (Fig. 1a) [5], the drive is capable of producing higher torque.

Current control during six-step voltage generation is problematic due to highly distorted current waveforms and a discontinuous set of available voltage vectors. Most control solutions disable the direct- and quadrature-current controllers upon switching to six-step mode, and activate a simplified control scheme that relies on look-up tables [6][7]. This allows for setting the angle of voltage vector (Fig. 2) in d-q

coordinates that corresponds to the reference torque at the actual drive speed. Nevertheless, deriving the look-up requires numerous assumptions including i.e. steady-state operation, constant DC-bus voltage, negligible influence of stator resistance etc. Most recent papers focus on decreasing the impact of these assumptions on control properties. Reference [7] introduces a modified control scheme that includes an additional control loop that uses DC-bus voltage feedback. The modified control is robust to changes in inverter input voltage, which is important in battery-powered drives, e.g. vehicle drives. Authors of [8] advise to set the reference voltage angle in a specific coordinate frame, instead of using the standard d-q frame. Setting the voltage in the proposed n-t reference frame minimizes the cross-coupling effect between motor torque and flux, so it provides better control stability. In turn, article [9] presents an approach that sustains the d-q current controllers during six-step operation. This requires numerous amendments in the control algorithm, but allows for regulating the instantaneous currents, so the dynamic properties of such a drive are superior.

Microprocessor-based implementation of the control algorithm is featured by discrete instants of output voltage update, both in linear modulation region and in six-step mode. The fundamental frequency of inverter output voltage increases proportionally to rotor speed; hence, the ratio between the update frequency and the fundamental frequency decreases with speed. When this ratio becomes small and if it is not an integer, the output voltage becomes distorted and motor currents consist of notable subharmonics. To avoid this, various synchronized pulse width modulation (PWM)
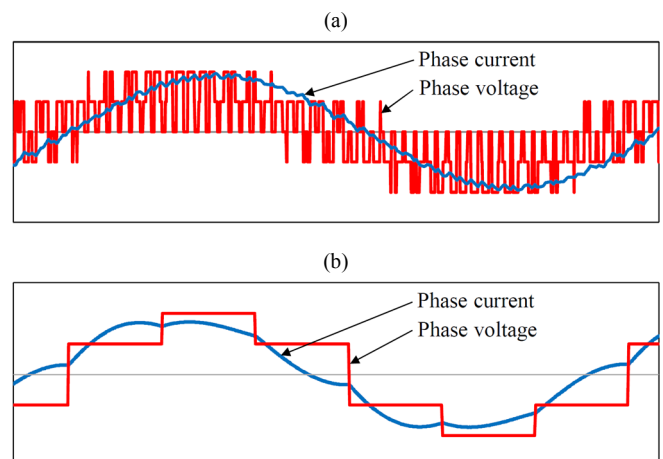

(a)

(b)

Fig. 1. Waveforms of motor phase voltage and current for:
(a) pulse voltage modulation; (b) six-step voltage generation

methods were introduced in order to maintain a round ratio between the update frequency and the fundamental frequency [10][11][12].

The focus of synchronized voltage generation is set on PWM operation. As described in the following section, this problem applies also to six-step operation. However, the synchronization of the six-step voltage must include different conditions than synchronized PWM. This paper proposes a comprehensive scheme to synchronized voltage generation dedicated for six-step operation of PMSM drive. By simulation and experiment, it is proven that the proposed scheme substantially decreases the torque ripples and subharmonic content of motor current.

II. SIX-STEP CONTROL

A simplified diagram of discrete six-step control of a PMSM drive is presented in Fig. 3. For simplicity, the control loops used in voltage modulation region are not included in the figure. In six-step mode the modulus of motor voltage vector $\underline{v}$ is fixed at 2/3 of the DC-bus voltage, so only the angle of this vector can be regulated. Hence, the control algorithm derives the angle v_{dq} of the voltage vector (Fig. 2) that corresponds to the reference torque at actual drive speed ω. Depending on the particular algorithm, other feedback signals may be used, as marked with dashed lines in Fig. 3. The optional feedback includes: inverter input voltage u_{DC}, motor phase currents i_A, i_B, i_C and rotor position θ.

The angle v_{dq} is expressed in the rotating d-q reference frame, so it must be transformed into the stationary frame in order to be used for inverter control. The sampled rotor angle θ changes quasi-continuously, so the angle v_{ABC} increases smoothly. However, in six-step mode only the fundamental inverter states can be used and this translates into the following set of possible voltage vector angles v_{ABC}: 0°, 60°, 120°, 180°, 240°, 300°. Selecting the angle nearest to the reference v_{ABC} assures that the fundamental component of the generated voltage is in phase with the reference corresponding to the quasi-continuously rotating vector.

Microprocessor implementation causes distinctive discrete control events, which are associated with the hardware up-down counter, whose state corresponds to the
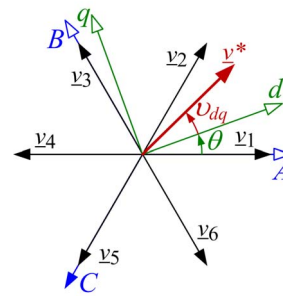

Fig. 2. Reference voltage vector $\underline{v}^*$ in rotating d-q and stationary ABC reference frames

carrier signal used in PWM [13]. Although PWM is not used in six-step, the counter still determines the instants of feedback sampling and voltage update, so the duration of control cycle T remains unchanged. The control algorithm is executed between current sampling and voltage update instants, as a part of interrupt service routine. Consequently, the update rate of the six-step voltage is equal to the switching frequency of PWM, which is typically selected between 500 Hz and 20 kHz, depending on drive rated power. In turn, the fundamental frequency of inverter output voltage may reach a few hundreds of hertz in high-speed drives. Therefore, in high-power drives or in high-speed drives the ratio between the update frequency and the fundamental frequency may decrease to 10 or less [10]. Following the studies on synchronized PWM, if this ratio becomes small the update frequency should be varied in a way that the value of update-to-fundamental frequency ratio sustains an integer, as this minimizes subharmonic content of the output voltage. Nevertheless, fulfilling this requirement is not enough for minimizing the negative impact of discrete control on drive performance in six-step mode, which is explained below.

Forming the six-step voltage requires that all the six voltage steps have equal duration. This problem is presented in Fig. 4a for an exemplary case of update-to-fundamental frequency ratio of 23. The duration of each step must be a multiple of control cycle T, so for the considered case one of the steps is shorter than the others. Thus, if the number of updates per voltage period is low, the output voltage is notably distorted.
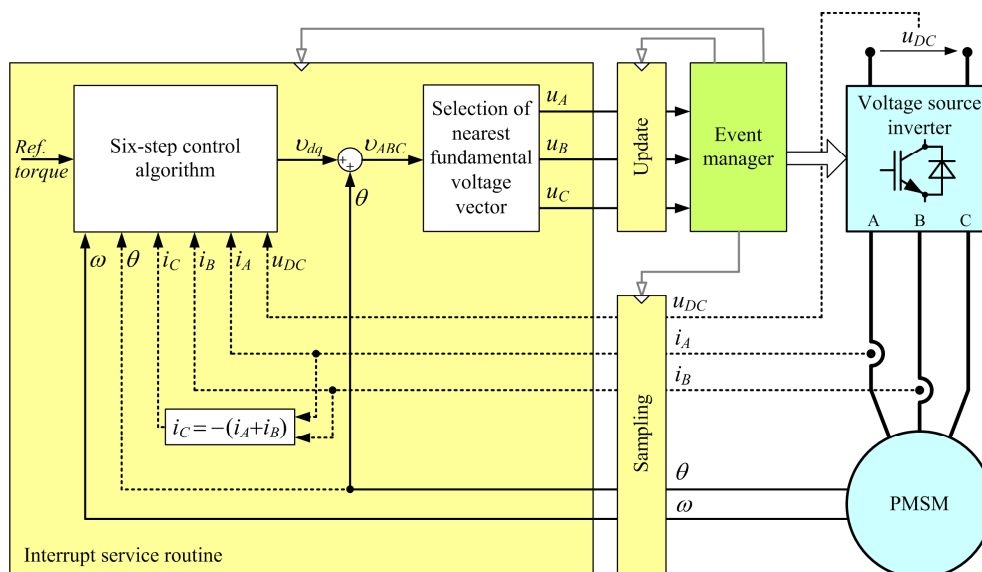

Fig. 3. Simplified scheme of microprocessor-based six-step control of PMSM drive

Another synchronization-related problem relates to following the reference angle υ_{ABC} of voltage vector, which is set by the control algorithm. As presented in Fig. 4b, the discrete update may introduce a time shift ΔT between the reference and output voltage, whose value is generally considered random. This time shift translates into a phase lag of the fundamental component of output voltage. Moreover, unsynchronized updates cause that the voltage phase may change in a step manner. To avoid this, the instants of voltage update should be synchronized with the intended transients in the output voltage, i.e. they should occur when υ_{ABC} crosses the values of 30°, 90°, 150°, 210°, 270°, 330°.

III. PROPOSED SYNCHRONIZATION SCHEME

The guidelines for voltage synchronization during six-step, which were formulated in the previous section, are included in the proposed synchronization scheme shown in Fig. 5. Equations used by the synchronization scheme are provided in the figure and commented below.

The scheme sets the duration $T^{[k+1]}$ of the forthcoming control cycle by adding two components. First component $T_{int}^{[k+1]}$ is computed in order to set a certain integer number n of update cycles in the fundamental voltage period. The computation assumes that the rotor speed ω is constant within the control cycle. The $T_{int}^{[k+1]}$ component constitutes a major part of the final outcome $T^{[k+1]}$ from the synchronization algorithm.

The number n must be a multiple of 6. Its value directly impacts the control cycle duration $T^{[k+1]}$, which must be long enough for the execution of control algorithm. On the other hand, overextending the control cycle duration $T^{[k+1]}$ has a negative impact on dynamic properties of the torque control [14]. Hence, the number n should be selected as a compromise, considering both of the above-discussed impacts. This may require changing the number n in accordance to the actual speed (Fig. 6), if the six-step operation covers a relatively wide range of operational speeds.

The second component of the duration $T^{[k+1]}$, named $\Delta T_{corr}^{[k+1]}$, aims at adjusting the instants of updates, so that they become synchronized with the intended instants of inverter switching. In other words, this component cancels the unintentional phase shift between output and reference voltage. The computations start with estimating the rotor position $\theta_{Tint}^{[k+1]}$ at the next update. This is carried out based on the assumption that $T^{[k+1]} = T_{int}^{[k+1]}$. Next, the angular error $\Delta\theta^{[k+1]}$ between the estimated position and the position that corresponds to the desired rotor angle upon switching is computed. The modulo operation is used for this purpose, so
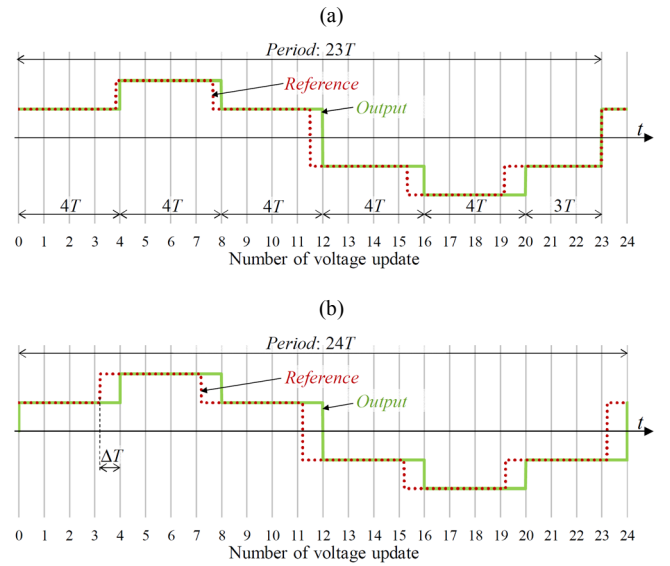

(a)

(b)

Fig. 4. Considered errors of generating six-step voltage:
(a) voltage distortion; (b) delay that translates into phase shift

TABLE I. PARAMETERS OF HIGH-SPEED TRACTION PMSM DRIVE

Parameter	Value
Control (PWM) frequency f	7.5 kHz or variable
Rated phase current I_r	8.75 A
Rated line-to-line voltage U_r	400 V
Rated speed ω	630 rad/s
Number of pole pairs	8
Stator resistance R	1.54 Ω
Stator inductances L_d, L_q	9.2 mH, 29.9 mH
Permanent magnets flux linkage ψ_f	465 mWb

the result of computation is positive or zero. As the error should express the angular difference between $\theta_{Tint}^{[k+1]}$ and the closest desired angle, the counter-domain of the modulo operation is shifted to $\langle-\pi/n, \pi/n)$. The angular error is next transformed into time shift ΔT that drives the P-type controller, whose gain is set below 1. Additionally, the output of the controller is limited to approximately 10% of T_{int} to assure smooth influence of ΔT_{corr} on the final output $T^{[k+1]}$ from the algorithm. This assures stable operation upon sudden changes of the reference angle υ_{ABC}.

As the idea behind the proposed scheme is to switch the inverter's transistors synchronously to the specific rotor angular positions, a special attention should be focused on rotor position measurement. A lag due to processing of rotor
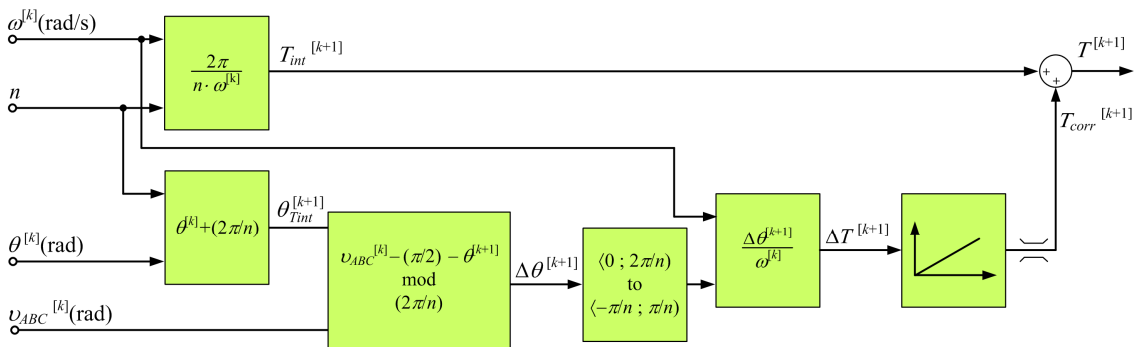

Fig. 5. Scheme of cycle-duration control algorithm for synchronized six-step voltage generation

position transducer's signals must be compensated. This is essential when using a resolver and resolver-to-digital converter. It is also possible to apply high-performance rotor position estimation methods [15][16].

IV. VERIFICATION

Verification was carried out for an exemplary 5-kW traction PMSM drive, which parameters are given in Table I. The synchronization algorithm from Fig. 5 was preprogrammed into the drive's controller. The number of updates n within the fundamental output voltage period depends on the speed-range, as shown in Fig. 6. As traction drives operate both in propelling and regenerative braking regimes [17], the relation between n and rotor speed was presented also for decelerating. The verification aims at comparing the synchronized and unsynchronized six-step voltage generation in terms of electromagnetic torque ripples and motor currents subharmonics.

The ripples of electromagnetic torque are problematic for experimental evaluation, because the moment of inertia of the rotor makes it impossible to measure the high frequency components of torque using a shaft-mounted dynamometer. Hence, the torque ripples were evaluated using a simulation model, whose structure is presented in [18]. The results of a drive acceleration test are presented in Fig. 7. If synchronization is not applied (Fig. 7a), the ratio n smoothly decreases while the drive accelerates, and the torque ripples gain for certain values of n. In turn, for synchronized six-step voltage generation (Fig. 7b) the ripples are uniform.

The current waveforms, presented in Fig. 8, were recorded in the laboratory drive for the same rotor speed. Without synchronization (Fig. 8a) the current consists of a notable subharmonic, whose frequency is approximate 20-times
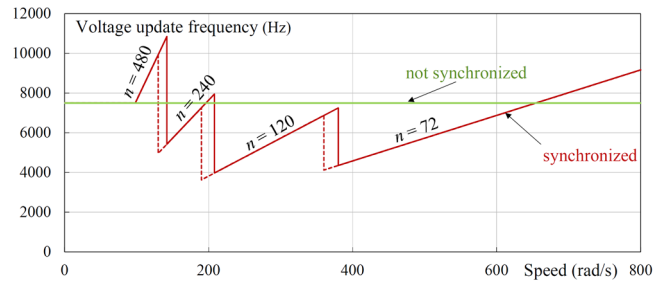

Fig. 6. Voltage update frequency vs. drive speed
(dashed line corresponds to decelerating)

smaller than the fundamental frequency. This undesirable subharmonic is not observable in the case of synchronized voltage generation depicted in Fig. 8b.

V. CONCLUSION

The positive effect of applying the proposed six-step synchronization was confirmed by simulation and experiment. In contrast to synchronized PWM, the input of the six-step synchronization scheme should include both rotor speed and reference angle of the voltage vector set by the torque control algorithm. Although the paper is focused on PMSM, similar problems of voltage generation occur in six-step controlled induction motor drives.

The verification was carried out using a drive whose minimal update-to-fundamental frequency ratio is 72. Even for this moderate ratio, the gain of using synchronized six-step voltage generation is clearly notable. As references report on using much lower update-to-fundamental frequency ratios, the benefits from the synchronized six-step may potentially be much more evident than it was demonstrated in this paper.
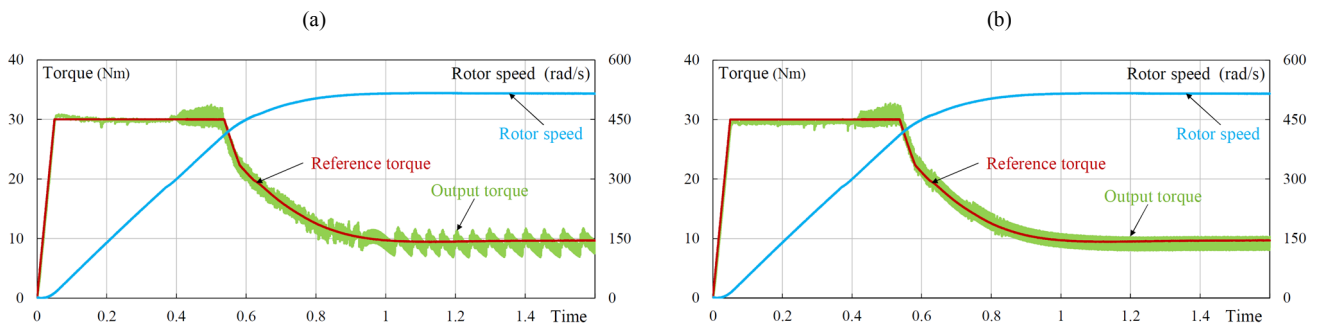
(a)

(b)

Fig. 7. Simulation results – torque ripples during acceleration: (a) without synchronization; (b) with proposed synchronization scheme
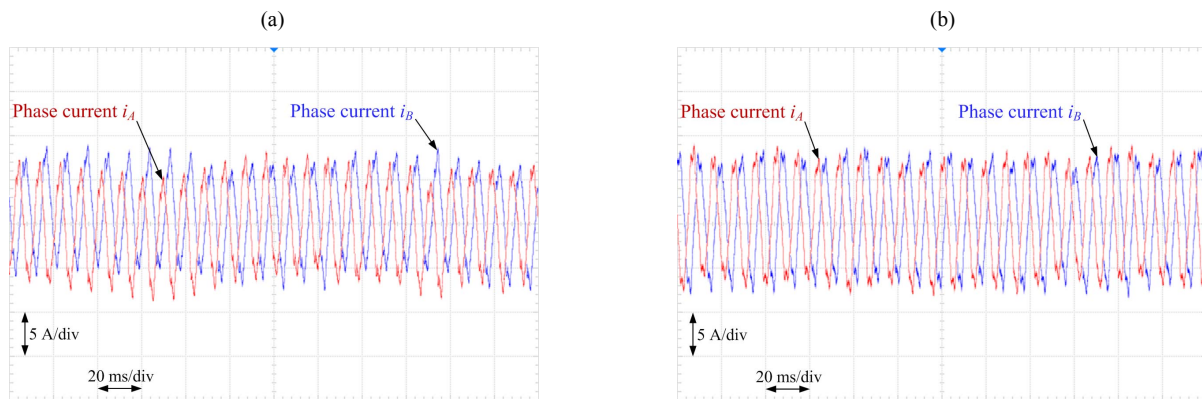
(a)

(b)

Fig. 8. Experimental results – motor phase currents: (a) without synchronization; (b) with proposed synchronization scheme

Moreover, cancelling the current subharmonics shall bring a positive impact in closed-loop current control algorithms, which have been recently proved superior in comparison to voltage-angle control.

REFERENCES

[1] J. Wang, J. Wu, C. Gan, and Q. Sun, "Comparative study of flux-weakening control methods for PMSM drive over wide speed range," in *2016 19th International Conference on Electrical Machines and Systems (ICEMS)*, 2016.

[2] A. El-Refaie and M. Osama, "High specific power electrical machines: A system perspective," in *2017 20th International Conference on Electrical Machines and Systems (ICEMS)*, 2017.

[3] L. Jarzebowicz, K. Karwowski, and W. J. Kulesza, "Sensorless algorithm for sustaining controllability of IPMSM drive in electric vehicle after resolver fault," *Control Engineering Practice*, vol. 58, pp. 117–126, Jan. 2017.

[4] T. Schoenen, A. Krings, D. van Treek, and R. W. De Doncker, "Maximum DC-link voltage utilization for optimal operation of IPMSM," in *2009 IEEE International Electric Machines and Drives Conference (IEMDC)*, 2009, pp. 1547–1550.

[5] A. Anuchin, F. Briz, D. Shpak, and M. Lashkevich, "PWM strategy for 3-phase 2-level VSI with non-idealities compensation and switching losses minimization," in *2017 IEEE International Electric Machines and Drives Conference (IEMDC)*, Miami, FL, USA, 2017.

[6] P. Lin and Y. Lai, "Voltage Control Technique for the Extension of DC-Link Voltage Utilization of Finite-Speed SPMSM Drives," *IEEE Transactions on Industrial Electronics*, vol. 59, no. 9, pp. 3392–3402, Sep. 2012.

[7] I. Ralev, T. Lange, and R. W. D. Doncker, "Wide speed range six-step mode operation of IPMSM drives with adjustable dc-link voltage," in *2014 17th International Conference on Electrical Machines and Systems (ICEMS)*, 2014, pp. 2987–2993.

[8] Y. Matsuki and S. Doki, "High response voltage phase torque control of IPMSM for both linear and over-modulation range of inverter," in *2017 19th European Conference on Power Electronics and Applications (EPE'17 ECCE Europe)*, 2017.

[9] Y.-C. Kwon, S. Kim, and S.-K. Sul, "Six-Step Operation of PMSM With Instantaneous Current Control," *IEEE Transactions on Industry Applications*, vol. 50, no. 4, pp. 2614–2625, Jul. 2014.

[10] V. Oleschuk and F. Barrero, "Standard and Non-Standard Approaches for Voltage Synchronization of Drive Inverters with Space-Vector PWM: a Survey," *International Review of Electrical Engineering (IREE)*, vol. 9, no. 4, pp. 688–707, Aug. 2014.

[11] S. K. Sahoo and T. Bhattacharya, "Rotor Flux-Oriented Control of Induction Motor With Synchronized Sinusoidal PWM for Traction Application," *IEEE Transactions on Power Electronics*, vol. 31, no. 6, pp. 4429–4439, Jun. 2016.

[12] M. Shafi, J. Peter, and R. Ramchand, "Space vector based synchronized PWM strategies for field oriented control of VSI fed induction motor," in *2016 IEEE International Conference on Power Electronics, Drives and Energy Systems (PEDES)*, 2016, pp. 1–5.

[13] L. Jarzebowicz, "Error analysis of calculating average d-q current components using regular sampling and Park transformation in FOC drives," in *2014 International Conference and Exposition on Electrical and Power Engineering (EPE)*, 2014, pp. 901–905.

[14] T. Tarczewski and L. M. Grzesiak, "High precision permanent magnet synchronous servo-drive with lqr position controller," *Przeglad Elektrotechniczny*, vol. 85, no. 8, pp. 42–47, 2009.

[15] K. Urbanski, "A new sensorless speed control structure for PMSM using reference model," *Bulletin of the Polish Academy of Sciences Technical Sciences*, vol. 65, no. 4, pp. 489–496, 2017.

[16] F. Wilczynski, M. Morawiec, P. Strankowski, J. Guzinski, and A. Lewicki, "Sensorless Field Oriented Control of Five Phase Induction Motor with Third Harmonic Injection," in *2017 11th IEEE International Conference on Compatibility, Power Electronics and Power Engineering (CPE-POWERENG)*, pp. 392–397.

[17] M. Bartłomiejczyk and S. Mirchevski, "Reducing of energy consumption in public transport — Results of experimental exploitation of super capacitor energy bank in Gdynia trolleybus system," in *2014 16th International Power Electronics and Motion Control Conference and Exposition*, 2014, pp. 94–101.

[18] L. Jarzebowicz and S. Mirchevski, "Modeling the impact of rotor movement on non-linearity of motor currents waveforms in high-speed PMSM drives," in *2017 19th European Conference on Power Electronics and Applications (EPE'17 ECCE Europe)*, 2017.